Clays and Clay Minerals, Vol. 58, No. 4, 486–500, 2010.

MODELING OF THE THERMOHYDRODYNAMIC AND REACTIVE BEHAVIOR OF COMPACTED CLAY FOR HIGH-LEVEL RADIONUCLIDE WASTE-MANAGEMENT SYSTEMS

RICARDO JUNCOSA[1,*], VICENTE NAVARRO[2], JORDI DELGADO[1], AND ANA VÁZQUEZ[1]

[1] Civil Engineering School, University of La Coruña, Campus de Elviña s/n, 15192, A Coruña, Spain
[2] Civil Engineering School, University of Castilla-La Mancha, Avda. Camilo José Cela s/n, 13071, Ciudad Real, Spain

Abstract—Bentonite is often proposed as an engineered-buffer material in high-level radionuclide waste-management systems. For effective design of the barrier that will provide protection over the long time periods required, the physical/thermal/chemical processes taking place in the barrier material must be understood thoroughly. These processes, which interact, include the flow of water and gas, the flow of heat, and the transport and reaction of chemical constituents. The purpose of this study was to better understand the processes that occurred in a small-scale experiment within a confined bentonite space. A conceptual and mathematical model (*FADES-CHEM*) was built in order to simulate the results of an experiment conducted in 2000, and thereby to gain a better understanding of the controlling processes. In that experiment, a block of compacted bentonite was placed in an air-tight cell and subjected, for 6 months, to simultaneous heating and hydration from opposite sides. The bentonite block was then sliced into five sections each of which was then analyzed in order to obtain a series of physicochemical parameters illustrating the changes that had occurred. Before modeling, the chemical composition of the bentonite pore waters was restored in order to account for different processes such as gas outgassing and cell cooling. Modeling indicated that gas-pressure build up was a relevant process when computing the saturation of bentonite, and the computations in the present study suggested that evaporation/condensation processes played a crucial role in the final distribution of the water content. Gas pressure and evaporation/condensation also affected the geochemical system, and the numerical model developed gives results that were consistent with the experimental values and trends observed. The model reproduced the results obtained and enable use at the repository scale and over longer time frames, provided that adequate data are available.

Key Words—Bentonite, Contaminant Transport, Multiphase Flow, Numerical Modeling, Reactive Transport.

INTRODUCTION

At the present time, the most feasible option for the safe disposal of high- and intermediate-level, long-lived nuclear waste is isolation in deep, stable, geological formations (KASAM, 1995). Geological disposal was defined in the 1995 Collective Opinion of the Nuclear Energy Agency Radioactive Waste Management Committee (NEA, 1995) as a system that (1) "isolates the wastes from the biosphere for extremely long periods of time," and (2) "ensures that residual radioactive substances reaching the biosphere will be at concentrations that are insignificant compared, for example, with the natural background levels of radioactivity." High Level Waste (HLW) disposal facilities must also provide reasonable assurance that any risk from inadvertent human intrusion would be very small. To fulfil the above requirements, agencies in charge of HLW management and their associated research and development programs have developed the concept of engineered barrier systems (EBS), *i.e.* an integrated strategy coupling the containment properties of different engineering materials such as steel, copper, concrete, or geologic materials such as zeolite or clay bricks with the hydrogeochemical and transport behavior of different types of geological formations. Ensuring that an EBS will perform its desired functions requires the integration of site characterization information, data on waste properties, data on the engineering properties of potential barrier materials, *in situ* and laboratory testing, and modeling (EC, 2003).

One of the candidate materials to be utilized as an engineered barrier is bentonitic clay (Krumhansl, 1986). Bentonite possesses particular properties including very low permeability, expansion upon hydration, and a great capacity to retain and/or delay the migration of radioactive nuclides without undergoing major alterations. The physicochemical conditions of the waste (heat + radiation) may lead to changes in the mechanical, physical, and chemical properties of the clay barrier, however, causing modifications in hydraulic conductivity, porosity, and retention capacity. To cope with this multifaceted problem, different tests and experiments

* E-mail address of corresponding author:
rjuncosa@udc.es
DOI: 10.1346/CCMN.2010.0580404

have been developed in order to study, identify, and analyze the processes happening in and around the containment barrier (non-isothermal multiphase flow and solute reactive transport).

The analysis and modeling of multiphase flow and reactive transport in porous media have a well known history in the hydrocarbon research industry, geothermal engineering, energy production, and environmental studies. Among the computer codes developed so far, the family of codes derived from *TOUGH* and *TOUGH2* (Pruess, 1987, 1991) are worth noting. This group of codes solves the non-isothermal multiphase flow by applying a numerical scheme based on integrated finite differences and, among their capabilities, some of them have been set to take into account the transport and reaction of solutes (*i.e. TOUGH2-CHEM* – White, 1995; *TOUGHREACT* – Xu and Pruess, 1998). *MULTIFLO*, a code written by Lichtner *et al.* (1996), was derived from the coupling of *METRA* (which solves the flow in finite differences) and *GEM* (a transport + chemical reactions simulator) and has capabilities similar to those mentioned earlier. Some other popular codes such as *3DHYDROGEOCHEM* (Cheng and Yeh, 1998) or *NUFT* (Nitao, 1998) can be added to this list. Within the realm of soil mechanics, multiphase flow codes have been widely employed: *CODE-BRIGHT* (Olivella, 1995), *COMPASS* (Thomas and He, 1997), and *FADES-CORE* (Juncosa, 2001).

FADES-CHEM was used in the present work – a code that was developed from *FADES-CORE*, including new constitutive thermo-hydrodynamic and chemical laws. In turn, *FADES-CORE* was developed from the integration and improvement of two less well known codes: *FADES* (Navarro, 1997; Navarro and Alonso, 2000) and *CORE-LE* (Xu, 1996). The thermo-hydraulic and geochemical models of the cell developed so far are one-dimensional models (Juncosa *et al*., 1999). In the present study the processes which occurred in a complex multiphase heating and hydration experiment (thermo-hydraulic cell) were studied, taking into account experimental data. *FADES-CHEM* was developed to reproduce the 3-D behavior of the material making up the containment barrier. Details of developments of the modeling of the thermo-hydraulic cell can be found in EC (2000) and Juncosa *et al.* (2003). These will provide a better understanding of the coupled interactions happening within the clay barrier.

CONCEPTUAL MODEL AND NUMERICAL FORMULATION

The porous medium can be satisfactorily represented by three distinct phases: (1) liquid (consisting of water, dissolved gases, and a number of aqueous species); (2) gaseous (made up of steam and 'dry air,' *i.e*. a fictitious species which encompasses all the gaseous species except for water vapor); and (3) bulk solid (composed of different mineral phases). To model the flow through the interconnected porosity of this multicomponent-multiphase domain, an advective/dispersive formulation was adopted (Juncosa, 2001; Xu, 1996). For both liquid and gas, the advective flow is described by a generalized Darcy's equation. Following Navarro and Alonso (2000), the intrinsic permeability functions for the liquid and gas phases are not the same in the model. The relative permeability of the liquid and gas depend on fluid saturation: When liquid saturation is less, the relative permeability of the gas is greater, whereas for the liquid it is less. Thus, two independent functions are needed to model relative permeability, and, according to Scanlon *et al.* (2002), they do not total one. In order to relate the relative permeability of liquid and gas to saturation, a number of expressions have been introduced. To describe water retention, the Van Genuchten (1980) formulation is widely used, but other expressions are also available in the literature. Dispersion is quantified using Fick's law of diffusion. If no significant gas flow takes place, the gas mechanical dispersion tensor can be safely overlooked (Gens *et al*., 1998), and a constant dispersion coefficient corresponding to the molecular diffusion of vapor in air can be assumed (Pollock, 1986).

The mass-balance equations are expressed for the porous medium as a whole (Pollock, 1986). The compositional approach (Panday and Corapcioglu, 1989) is adopted to establish the water and air mass-balance equations. Equilibrium restrictions are introduced for the concentration of water vapor in gas and dissolved air in water. The psychrometric law (Edlefsen and Anderson, 1943) is, hence, applied to define the vapor density, while Henry's law is used to compute the amount of dissolved air in the liquid. Therefore, liquid and gas pressures are the state variables in an isothermal flow problem. In a non-isothermal problem, local thermal equilibrium between the soil constituents is assumed. The temperature is, therefore, postulated to be a new state variable, and only one equation of enthalpy is needed. In the enthalpy balance equation, which has the same structure as the mass-balance equations, the heat flux includes both conduction and advection. The bulk thermal conductivity is calculated by default using a volumetric weighted mean value of the dry and saturated thermal conductivities of the modeled medium (Table 1).

FADES-CHEM considers a transport equation for each chemical component (or primary species) (Juncosa, 2001; Xu, 1996) while the transport phenomena considered are advection, molecular diffusion, and hydrodynamic dispersion. In the last case, the solute mechanical dispersion tensor has been formulated following Bear (1972).

In the definition of the chemical system, the model uses an approach similar to those available in many other geochemical modeling codes (*EQ3NR* – Wolery, 1992; *PHREEQC* – Parkhurst, 1995; *MINTEQA2* – Allison *et*

Table 1. Flow and transport parameters used in the model.

Parameter	Value/expression	Units	Source
Intrinsic permeability of liquid, K_l	$1\times10^{-20}\ (\varphi/0.407)^3\cdot(0.593/(1-\varphi))^2$	m^2	EC (2000), Nguyen *et al*. (2005)
Relative permeability of liquid, κ_l	$(S_l)^3$	dimensionless	EC (2000), Nguyen *et al*. (2005)
Intrinsic permeability of the gas, K_g	5×10^{-11}	m^2	EC (2000), Nguyen *et al*. (2005)
Relative permeability of the gas, κ_g	$(1-S_l)^3$	dimensionless	EC (2000), Nguyen *et al*. (2005)
Vapor tortuosity, τ_v	$\tau_v = \theta_l^{7/3}/\phi^2$	dimensionless	Simunek and Suarez (1994)
Molecular diffusion of vapor in air, D_m^v	$D_m^v = 5.9\times10^{-6}(T^{2.3}/P_g)$	m^2/s; T in K; P_g in Pa	Navarro and Alonso (2000)
Retention curve, S_l	$\left(1-\frac{\psi}{1100}\right)/\left(1+(0.05\cdot\psi)^{1.22}\right)^{0.18}$	$\psi = P_g - P_l$ (suction) in Pa	Van Genuchten (1980) EC (2000)
Thermal conductivity	$\Lambda = \Lambda_d^{1-\phi}\cdot\Lambda_S^{\phi}$	Subscripts: d: dry; S: saturated	EC (2000)
Clay specific heat	c_s : 835.5	J/K kg	EC (2000); Lide (1997)
Air Henry's constant	10^4	MPa	Navarro and Alonso (2000)
Vapor reference density, $\rho_0^v(T)$	$\exp(0.06374T - 0.0001634T^2)/194.4$	T in °C	Mayhew and Rogers (1976)
Diffusion coefficient at 293 K, D_0	2×10^{-10}	m^2/s	Li and Gregory (1974); see text
Dependence on temperature of D_0	$D_0(T) = D_0(T_0)\frac{T}{T_0}\frac{\mu_1(T_0)}{\mu_1(T)}$	m^2/s	EC (2000)
Longitudinal dispersivity, α_L	0.001	M	This work
Tortuosity, τ	$\tau = \theta_l^{7/3}/\phi^2$	dimensionless	Simunek and Suarez (1994)

al., 1991; *The Geochemist's Workbench*® – Bethke, 1994; among others). In short, the chemical composition of the system is given according to selected primary species which, when combined according to mass action equations, results in a bundle of aqueous secondary species that comprise the speciation of the aqueous system. In order to compute the distribution of aqueous species, the degree of saturation with respect to different minerals, partial pressures of gases, *etc*., is required in order to calculate the total aqueous concentrations for each component and to establish the corresponding mass-balance and mass-action equations. Similarly, the amount of each component linked to the solid matrix *via* ion exchange and/or adsorption are computed using analogous restrictions. A comprehensive description of the numerical formulation of geochemical reactions implemented in *FADES-CHEM* can be found in Xu and Pruess (1998) and Juncosa *et al*. (2001). The transport equations operate on a component basis while the rest of the aqueous species are derived from the mass-action/mass-balance constraints. The sink/source term of each transport equation accounts for the mass of component sequestered/delivered to the solution according to a series of geochemical processes: dissolution/precipitation of minerals, ion exchange, and adsorption (Xu, 1996).

'Spatial discretization' in *FADES-CHEM* is based on the Bubnov-Galerkin Finite Element Method (BG-FEM). However, the fluxes found using the BG-FEM are not continuous for discontinuous coefficient problems (Wang *et al*., 2003), one of the reasons why reactive transport modelers tend to prefer the finite-volume method, which is always mass conservative (Mayer *et al*., 2002). If the BG-FEM is applied, a mesh refinement at the contact between heterogeneous materials will be required to avoid relevant local mass-balance errors, though it does lead to increased computing costs. The errors are minimized by *FADES-CHEM* through the use of mass conservative schemes in accordance with Milly (1985) and Celia *et al*. (1990) to integrate the temporal derivatives of the mass-balance equations.

After 'discretization,' the non-linear equations obtained are solved using a 'staggered' scheme, *i.e.* first the coupled equations of flow (liquid, gas, and enthalpy) are solved, and then the code proceeds to solve the reactive transport equations. In both cases, Newton's method with an exact Jacobian matrix is employed. The rate of evaporation/condensation was calculated by formulating the mass balance equation of water through its splitting into two mass-balance equations: one for the liquid and one for the gaseous phase. Once the transport of reactive species was solved, the change in liquid density was evaluated. If the variation was >2%, the flow equations were solved again before computing the solution of the transport/reaction equations again.

FADES-CHEM offers three methods of coupling the reaction and transport terms: (1) the sequential (fully)

iterative approach (SIA); (2) the sequential (partially) iterative approach (SPIA), where iterations are only performed in those nodes where the prescribed tolerance criterion for transport is not satisfied; and (3) the sequentially non-iterative approach. All of these are documented in Steefel and Macquarrie (1996) and Xu (1996). The thermohydraulic cell described in this text was modeled using the SIA approach. *FADES-CHEM* has been verified with analytical solutions and comparable codes, including benchmark exercises with *TOUGHREACT* (Xu and Pruess, 1998; Juncosa *et al*., 2001).

AXISYMMETRIC 3-D MODELING

Description of the experiment

The aim of the EU-funded FEBEX Project (Full-scale Engineered Barriers Experiments) was to demonstrate the technical feasibility and study the behavior of near-field components of a high-level radioactive waste repository in crystalline rock (EC, 2000). The project consisted of an "in situ" test, a "mock-up" test, and a series of complementary laboratory tests (small-scale heating and hydration tests) as well as modeling work (Cuevas *et al.*, 1997). In short, several layers of bentonite were compacted inside a stainless steel, water-tight cylinder with the aid of a Proctor hammer in order to achieve a prescribed initial dry density (Villar *et al*., 1995, 1996; Villar and Lloret, 2004; Cuevas *et al*., 1997; EC, 2000; Fernández *et al*., 2004). At the bottom of the cell, two hydration ports allowed the passage of deionized water from a reservoir to the bentonite (Figure 1). The water was injected with an automatic pump at a constant pressure of 1 MPa throughout the duration of the experiments. At the upper part of the cell and in contact with the bentonite, a brass flat heater was kept at a constant temperature of 373 K. The cell was equipped with a data-acquisition system that recorded the input from 12 thermocouples located at four heights and three different radial distances inside the bentonite. The clay block was simultaneously hydrated and heated in order to simulate the processes taking place in a bentonite barrier caused by heat dissipation from a radioactive source in a location below the water table.

The experiment modeled corresponded to the cell test, which was kept running for 4394 h (~6 months). The total volume of water that entered was 486 cm^3 and the flow rate was unknown (EC, 2000). At the end of the experiment, the cell was decommissioned and the bentonite block was halved. Each half was then sliced into five sections (section 1 was that in contact with the heater and section 5 was at the hydration end) parallel to the heater plate. One half was used to obtain a series of physicochemical parameters (water content, density distribution, porosity, leaching tests, exchange complex, and CEC) while the second half was employed to analyze the final chemical composition of the pore waters (pH, TIC, Cl, SO_4, Ca, Mg, Na, and K).

The chemical composition of the pore waters was obtained by applying a compression technique (squeezing) which is a procedure that involves the expulsion of pore fluids from the soil when submitted to compression. At that time, the squeezing technique was the most reliable method to obtain hydrochemical information

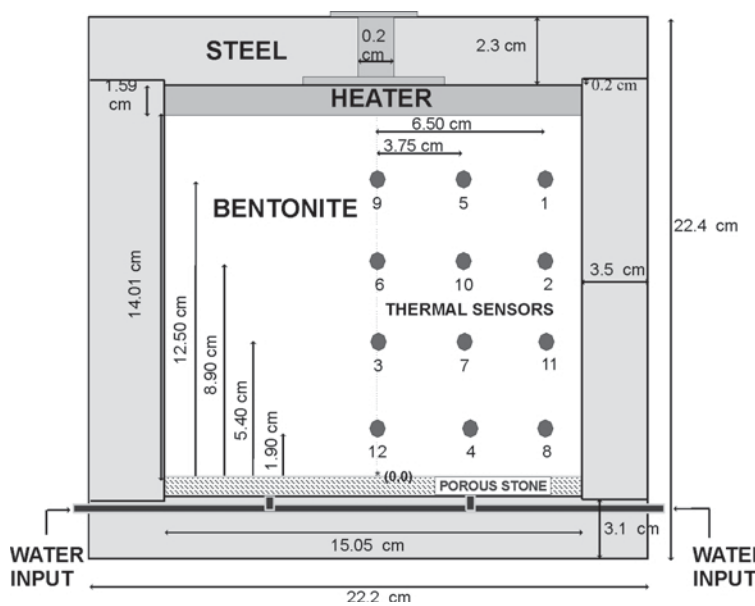

Figure 1. Schematic diagram of the thermohydraulic cell. Also indicated are the dimensions and the location of the thermocouples and water injection ports. Modified after Cuevas *et al*. (1997).

from low-permeability media, although some drawbacks must be taken into account (Fernández *et al*., 2004). Among others, NEA (2000) points to effects such as: (1) the eventual dilution associated with the release of water from the double layer of clay minerals; (2) potential membrane effects; (3) chloride exclusion; and (4) analytical difficulties due to the very small volumes of water sampled. All of these could be of relative importance at very high pressures (>70 MPa; Chillingarian and Riecke, 1968; Manheim, 1974) although they might introduce some uncertainty in the analytical determinations. Muurinen (2001) suggested a series of uncertainty values that can be used to assess the confidence bracket around each analytical determination (Table 2).

Due to the reduced size of the cell, the characteristics of the bentonitic material and the relatively high temperatures attained, at the time the experiment was performed no accurate method was available to record online any of the relevant geochemical parameters needed for modeling. Hence, values corresponding to intermediate times are not accessible and the results of the geochemical characterization (both solid and pore waters) could only be performed once the experiment was concluded.

Parameters and data

According to the geometry of the experiment, an axisymmetric-3D model was employed (Tables 1, 2, and 3). The solid density and dry density of the bentonite compacted in the cell were 2780 kg/m^3 and 1650 kg/m^3, respectively (Villar *et al*., 2005), and the initial average gravimetric water content was 11.2%, which corresponds to a degree of saturation of ~45%. Due to the *in situ* compaction of the bentonite, the initial porosity of the block may have been slightly variable, depending on the relative position inside the cell. For the sake of modeling, an average and constant porosity of 0.41 was assumed.

Water was injected into the cell at a constant pressure of 1 MPa and this was the constant pressure boundary condition selected for the hydration end of the cell. At the top of the cell (where the heater was located), an impervious-to-flux boundary condition was assigned.

The coupled effect of heat and the injection of water produced the redistribution of water inside the cell and both were recorded by the different water contents associated with each one of the bentonite slices analyzed at the end of the experiment. The water contents enabled the assessment of the thermohydraulic model.

Due to the air-tight design of the cell, the air contained in the pores of the bentonite before the injection of water (which was initially at an atmospheric pressure of 0.1 MPa) did not have the opportunity to leave the system and, therefore, a significant gas-pressure build-up was expected to take place throughout the saturation process. In order to cope with this situation, the coupled flow of the liquid and gas phases was computed.

Once the thermal steady state of the cell was attained, the temperature used along the heater/bentonite interface remained between 373 and 328 K and this was the temperature assigned as a boundary condition of the model to the heater side. On the injection side the temperature was fixed according to the monitored room temperature (*i.e*. 293 K). The calibration of the thermal model was accomplished by allowing heat, q_c, to be transferred from the cell toward the surroundings. From a numerical standpoint, this requires a mixed-type boundary condition that can be stated as $q_c = \alpha_T \cdot (T - T^*)$, where α_T = 821.6 W/K was the average value used, and T^* represents the temperature of the cell surroundings (293 K).

The molecular diffusion coefficients of the different solutes in water were assumed to be equal to those in pure water. Moreover, the diffusion coefficient, D_0, of all solutes present in the pore waters has an identical value and this was computed from the weighted-average values corresponding to the chemical species present in the system (Li and Gregory, 1974). However, in contrast to what happens with the molecular diffusion coefficient, dispersion coefficients are a function of the volumetric water content (Xu, 1996; Juncosa *et al*., 2003).

The water injected into the cell was neutral and deionized meaning that it did not contribute solutes to the bentonite although it promoted chemical reactions according to the time-dependent temperature, moisture, and derived compositional gradients. One of the most relevant geochemical processes expected to occur in the cell due to the flow of water not in equilibrium with the bentonite are ion-exchange reactions. The mineralogical characterization of the bentonite indicates the presence of some important trace minerals that participate in dissolution/precipitation reactions (EC, 2000; ENRESA, 2004). Among them, the most significant is calcite. Moreover, some newly formed mineral phases, such as anhydrite, were incorporated into the model as a potential sink/source of aqueous solutes owing to the possibility of their precipitation close to the heater following an important evaporation of the pore waters and dissolution due to the advance of the hydration front.

Semi-quantitative analyses of the bentonite (Pusch *et al*., 1999), based on the relative corrected areas of selected peaks from the XRD patterns (Moore and Reynolds, 1997), yielded an average mineralogical distribution of 96% dioctahedral smectite, 1.5% cristobalite, 1% quartz, 1% calcite, and trace amounts of K-feldspar and tridymite. The XRD patterns of the oriented and glycolated mounts revealed that it was actually an R = 0 mixed-layer illite/smectite (I/S), with 15% illite layers (Huertas *et al*., 2001; Pusch and Karnland, 1986).

The initial composition of the exchange complex of the bentonite employed in the cell tests is known (EC,

Table 2. Initial and final values corresponding to the pore-water chemistry phase, and selected physical parameters of the bentonite assayed in the thermohydraulic cell. Aqueous concentrations in molality; n/a: not analyzed. Numbers within brackets are uncorrected with respect to *P* and *T*. Leachable anions in 1:4 solid to water ratio.

Parameter	Initial	Section 1	Section 2	Section 3	Section 4	Section 5	Uncertainty [b]
Ca^{2+}	1.0×10^{-2}	n/a	(2.8×10^{-3})	$(2.3\times10^{-3})1.4\times10^{-3}$ [a]	$(2.7\times10^{-3})1.8\times10^{-3}$ [a]	$(5.9\times10^{-4})2.6\times10^{-4}$ [a]	±10%
Mg^{2+}	1.7×10^{-2}	n/a	2.8×10^{-3}	2.9×10^{-3}	3.2×10^{-3}	5.5×10^{-4}	±10%
Na^{+}	7.5×10^{-2}	n/a	3.8×10^{-2}	3.3×10^{-2}	3.1×10^{-2}	1.4×10^{-2}	±10%
K^{+}	1.2×10^{-3}	n/a	7.1×10^{-4}	5.9×10^{-4}	1.0×10^{-3}	1.0×10^{-4}	±25%
Cl^{-}	7.7×10^{-2}	n/a	2.3×10^{-2}	1.6×10^{-2}	1.4×10^{-2}	6.2×10^{-3}	±10%
SO_4	2.6×10^{-2}	n/a	1.2×10^{-2}	1.2×10^{-2}	1.3×10^{-2}	4.4×10^{-3}	±10%
HCO_3	1.0×10^{-3}	n/a	(2.8×10^{-3})	$(2.5\times10^{-3})6.0\times10^{-4}$ [a]	$(2.3\times10^{-3})6.2\times10^{-4}$ [a]	$(2.3\times10^{-3})1.4\times10^{-3}$ [a]	±20%
pH	8.0	n/a	n/a	(7.44) 8.14[a]	(7.30) 8.10[a]	(7.53) 8.47 [a]	±0.1 units
Ionic strength (M)	0.19	n/a	0.07	0.06	0.07	0.02	–
Charge balance (%)	0.5	–	5.2	2.7	1.4	0.8	–
Average temperature (ºC)	20	75	60	45	38	34	–
Leachable Cl (μmol/g)	19.3	630.2	66.2	25.4	27.2	17.3	–
Leachable SO_4 (μmol/g)	9.1	65.3	139.2	99.6	100.9	27.2	–
Leachable HCO_3 (μmol/g)	50.9	35.4	103.6	119.3	121.1	163.2	–
Porosity, ϕ	0.41	0.40	0.41	0.43	0.44	0.46	–
Dry density, ρ_d (kg/m^3)	1650	1610	1580	1530	1520	1460	–
Water content (%)	11.2	18.5	21.7	23.7	23.8	25.1	± 5 %
Calcite volume fraction (%)	0.01	–	–	–	–	–	–
Thickness (cm)	–	1.198	3.203	3.203	3.203	3.203	–

Notes: a: corrected for pressure. b: uncertainties after Muurinen (2001).

Table 3. Initial and final values of the exchange complex and cation exchange capacity, in meq/100 g of dry soil. Also indicated are the Gaines-Thomas-based selectivity coefficients, computed from Huertas *et al*. (2001).

Exchange complex	Initial	Section 1	Section 2	Section 3	Section 4	Section 5
Na^+	27±2	27.6±0.6	25.3±3.7	26.0±2.7	27.1±0.7	27.6±0.7
K^+	2±0.3	2.0±0.1	2.0±0.1	1.9±0.2	2.1±0.1	2.1±0.1
Ca^{2+}	50±2	52.8±1.3	49.3±1.5	48.6±7.2	53.1±2.6	51.2±3.7
Mg^{2+}	32±3	32.8±0.6	33.1±4.6	30.6±3.7	32.3±0.9	32.6±1.2
CEC	111±4	107.5±1.0	109.7±0.9	107.1±1.3	114.6±3.3	113.5±3.7

Exchange reaction	Selectivity coefficients
$Na^+ + 0.5Ca{-}X_2 \rightleftharpoons 0.5Ca^{2+} + Na{-}X$	0.25
$Na^+ + 0.5Mg{-}X_2 \rightleftharpoons 0.5Mg^{2+} + Na{-}X$	0.58
$Na^+ + K{-}X \rightleftharpoons K^+ + Na{-}X$	0.22

2000) while the corresponding selectivity coefficients (Gaines-Thomas convention) were computed from experimental isotherms performed with the bentonite (Huertas *et al*., 2001). Finally, in order to take into account the initial water content of 11.2%, the chemical composition of the pore waters of the bentonite was computed following the procedures and methods described by Fernández *et al*. (2000, 2004). The greatest computed ionic strength of the cell pore waters (0.07 molal; Table 2) is less than that corresponding to the initial pore water (~0.2 molal) and all of these are well within the applicability range of the extended Debye-Hückel formalism to compute aqueous activity coefficients.

Corrections to analytical data

The end-of-the-experiment analytical values are important because they are the only way to assess the success of the modeling process. A series of pressure and temperature corrections to the analytical data was, therefore, needed prior to carrying out a direct comparison with the model results (Table 2). The correction of pressure is important for the solubility and speciation of carbonates (Stumm and Morgan, 1981; Millero, 1982; Zilberbrand, 1999). Moreover, the eventual CO_2 out-gassing from the pore water sample, from the time it is extracted up to its final analysis, introduces additional uncertainties into the carbonate system (Pearson *et al*., 1978). Taking all the above into account, the pressure correction was based on two assumptions: (1) that the pore water remained in equilibrium with calcite throughout the extraction (from 0.1 MPa, after the end of the test, up to 64 MPa); and (2) that pH, under the experimental conditions, is independent of pressure. Thus, the effect of out-gassing at room pressure on the total dissolved carbonate (TIC) was accounted for by using the total analytical Ca concentration and pH and by computing TIC by means of the equilibrium with calcite (Kaufhold *et al.*, 2008). Next, the *SUPCRT92* code (Johnson *et al*., 1992) was used to correct the equilibrium constant of calcite and the relevant aqueous species to 64 MPa. All of these data were then entered into the *EQ3/6* software package (Wolery, 1992) to compute the composition of the pore fluid by subtracting the excess Ca and TIC associated with the pressure-enhanced solubility of calcite.

The second and quantitatively more important correction is related to temperature. Once the experiment was concluded, the heater was switched off and the hydration system was dismantled. After a few hours (the time needed for the safe manipulation of the cell), the clay block was extracted and processed rapidly in order to preserve its unaltered properties (water content, *etc*.). For practical reasons, however, the extraction of pore waters was performed once the slices were equilibrated to room temperature. Hence, for each slice, and in order to correct this effect, the average temperature derived from the steady-state thermal distribution of the corresponding slice-to-height relationship was entered into the *EQ3/6* software to re-equilibrate the available pressure-corrected pore-water compositions one by one.

Not all the slices could be corrected using the method described above. In fact, the availability of water decreased considerably as the heater was approached and recovery of any water from section 1 (that in contact with the heater) was impossible. Moreover, the amount of water delivered by section 2 was insufficient to perform the complete battery of analytical determinations (notably pH), which made accurate P and T corrections impossible.

The correction carried out affects the carbonate system in particular. Although the P and T effect on the exchange complex is assumed to be minimal, the lack of information rules out the possibility of making any consistent assessment and, in any case, such a correction would be less than the combined uncertainties associated with its analytical determination and the corresponding selectivity coefficients.

Thermohydraulic model

The model temperature distribution is consistent with the horizontally variable temperatures measured in each clay slice (Figures 2b, 3c). Due to the small amount of material available for the determinations, the reproducibility of the measurements on the gravimetric water content of each of the five half-slices of bentonite did

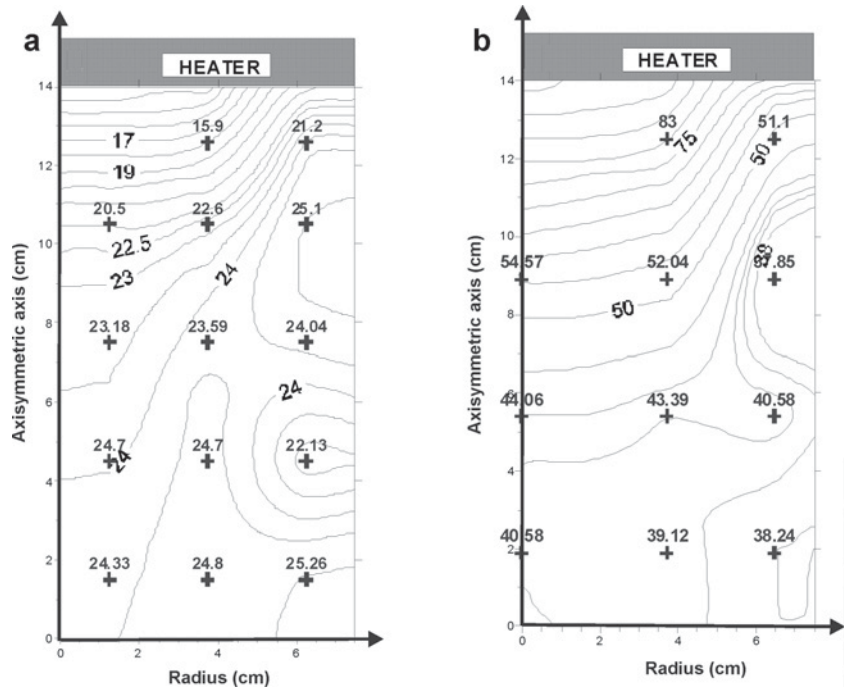

Figure 2. Experimental determinations (cross) and model results (black lines) at the end of the experiment: (a) gravimetric water content; (b) temperature.

not allow the assessment of the corresponding uncertainties. A 5% error bracket was, therefore, adopted, which is believed to be acceptable, taking into account that available data represent averaged values and that, owing to thermal effects, the moisture content may not have been homogeneous within each half-slice. On the other hand, the final gravimetric water content distribution computed by the model was compared with the distribution of experimental values (Figure 2a) and with experimental values of the corresponding slices (Figure 3a, 3b). The agreement between model and experimental data was good. As expected, the water content decreased close to the heater due to evaporation while in the zone adjacent to the porous stone the bentonite attained full saturation, corresponding to a water content of 25.5 wt.%. The vapor that formed in the vicinity of the heater was transported by diffusion and advection toward the cooler mid-zone of the cell. At that point, condensation took place (Figure 3d). Moreover, as the saturation front reached the proximity of the heater, owing to the existence of the hydraulic gradient caused by the entrance of water, evaporation occurred again. The model presents, therefore, the arrangement of a non-steady state flow cycle involving water and steam.

The associated values of the gas pressure are significantly greater than the initial atmospheric pressure of 0.1 MPa (inset in Figure 3a, 3b), though it features a rather flat shape, the only exception being the discontinuity observed near the saturation front. The final water content was significantly different, ignoring the effect of gas flow and pressure build-up.

Conservative/reactive transport models

The geochemical evolution of the cell is related to the processes triggered by simultaneous heating and hydration. The present study has focused on non-kinetically constrained reactions for a number of reasons: (1) the analytical data provide no information relative to the aqueous concentration of relevant components (*e.g.* Al, Fe,); (2) due to unavoidable characterization constraints, the chemical composition of the pore waters could not be measured in a continuous manner, and so the time-dependent evolution of each relevant component could not be tracked in time; and (3) other relevant data such as reactive surface areas are not available. The equilibrium processes were analyzed, therefore, to check whether kinetics played a significant role over the 6-month experimental period and for the chemical components and phases available. The research is currently limited to the study of the short term.

Conservative components. Taking into account the analytical constraints outlined earlier, the model results followed the experimental trends reasonably well (Figures 4–6). The larger discrepancies can be found in the vicinity of the heater where, in general, model concentrations were less than the experimental values.

Conservative components enabled a more in-depth examination of some of the features of the hydration process. The model predicts a sharp increase in concentrations of chloride near the heater due to the initial evaporation of the interstitial water of the bentonite (Figure 4a,b) creating a concentration gradient

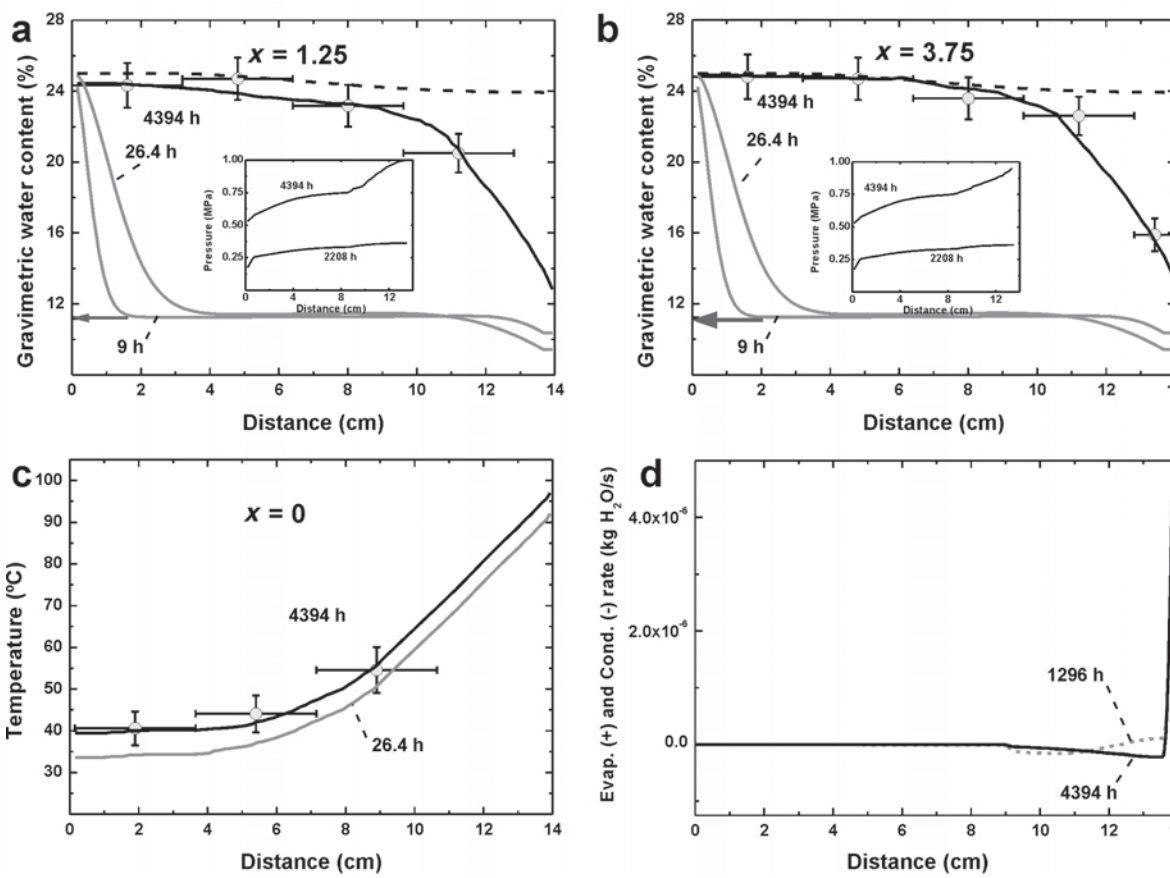

Figure 3. Experimental determinations and model results for different times (gray lines) and at the end of the experiment (black line). (a) Water-content distribution taking and not taking into account gas pressure (continuous and dashed lines, respectively) at $x = 1.25$ cm. The inset shows the gas-pressure evolution at two times. (b) Water-content distribution taking and not taking into account gas pressure (continuous and dashed lines, respectively) at $x = 3.75$ cm. The inset shows the gas pressure evolution at two times. (c) Temperature distribution at $x = 0$ cm. (d) Evaporation rate at two different times at $x = 0$ cm.

that triggers the diffusive transport of species away from the heater. Contrary to this, at the hydration end, the concentration of chloride tended to decrease due to the dilution and flushing (advective/diffusive transport) with distilled water. During the early stages, before the hydration front had reached the central area of the cell, the initial chloride concentration decreased slightly due to the condensation of water previously evaporated in the vicinity of the heater.

In order to verify the reliability of the model results and the utility of squeezed pore waters as an indicator of the final solution chemistry, the amounts of leachable chloride obtained from the five sections of bentonite analyzed were highly suggestive. The greater proportion of leachable chloride was located in section 1 (in contact with the heater; Table 2), consistent with the results. In fact, the amount of leachable Cl in that section was >30 times greater than the quantity in the untested bentonite, indicating an intensive process of evaporative re-concentration and solute transport. Concomitantly, the amount of leachable Cl diminished from section 1 to 5. The same tendency was observed in the squeezed waters. On the other hand, the initial chloride concentration of the pore water was greater than the value found in any of the sections but note that the initial water content of the bentonite at the beginning of the experiment was less than the content corresponding to any section after the experiment had finished. Another interesting point is that, as the experiment progressed, the domain affected by evaporation became more and more reduced (Figure 3d) suggesting that the saturation front had reached the area and more water was entering than was evaporating.

Reactive components. The general features described for chloride were present in the rest of the aqueous species analyzed (Figures 4c, 4d, 5b, 5e, 5f), although the shape of the corresponding profiles became slightly more complicated according to a series of chemical reactions affecting the total amount of any given component remaining in solution. This implies: (1) a substantial increase in concentration in areas near the heater;

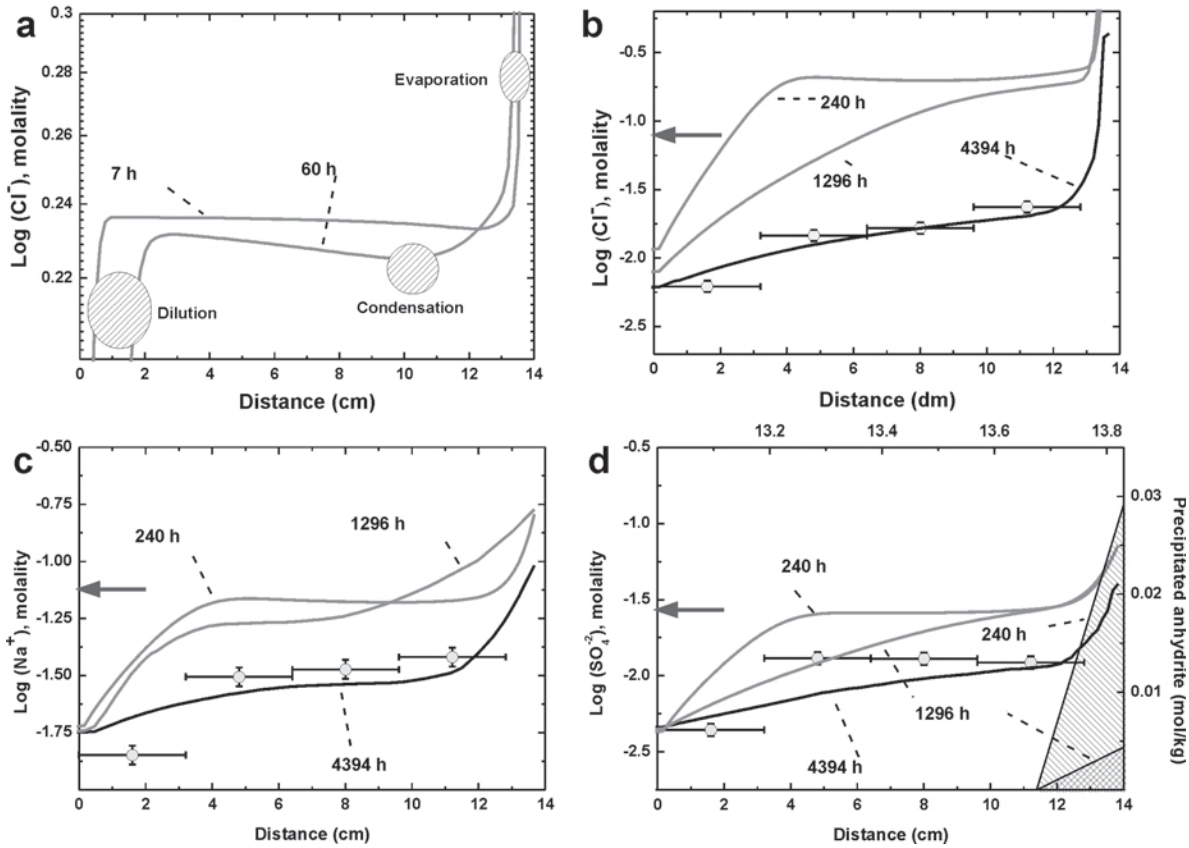

Figure 4. Experimental determinations and model results for different times (gray lines) and at the end of the experiment (black line). (a,b) Chloride concentration. (c) Na concentration. Arrows indicate the initial concentrations of the corresponding component. (d) Sulfate concentration. On the right-hand side of the plot, the amount of anhydrite precipitated at two different times.

(2) dilution in zones near the source of hydration due to the entrance of water; and (3) a slight dilution in the area where vapor condensation takes place at the early stages of the experiment. The concentrations of the different chemical species tended to decrease gradually near the heater due to the diffusion phenomenon and the arrival of the hydration front. The cations were also affected by exchange reactions with the clay and by the dissolution and precipitation of solid phases calcite and anhydrite.

The simultaneous heating and hydration of the cell triggers different processes, although they are coupled with thermal, mass transport, and equilibrium processes. At the beginning of the experiment, the sharp increase in temperature and the evaporative concentration of sulfate near the heater caused the pore-water solution to become saturated with respect to anhydrite, which precipitated (Figure 4d). As hydration proceeded, the initially precipitated anhydrite began to dissolve, and by the end of the experiment had completely disappeared. Accordingly, and in contrast to chloride, the leachable sulfate did not attain its greatest amount near the heater, but rather in the intermediate portion of the cell. The model, in this case, under predicted the aqueous concentration of sulfate slightly.

Calcite, the solubility of which decreases with temperature, behaved similarly to anhydrite (Figure 5d) and precipitated on the heater side but did not dissolve later. The precipitation of calcite caused the TIC concentration and pH to drop (Figure 5b,c). At that point, Ca increased in concentration due to the fact that the Ca/TIC ratio of the pore water was >1 and the evaporation/precipitation process favors the presence of this component in solution. On the other hand, on the hydration side a dissolution front of calcite began to move toward the heater (Figure 5d) over the course of the experiment, as more calcite-under-saturated water began to enter. The solubility product of the calcite constrains the concentration of Ca and TIC in solution, however. Because temperature increased as the heater was approached, calcite began to precipitate close to the base of the cell. Over the course of the experiment and as more water entered the cell, the leading edge of the calcite precipitation front and the rear of the calcite dissolution front moved toward the inner part of the bentonite block. Congruently, leachable TIC presented the greatest amounts in the intermediate parts of the cell, with a sharp rise in section 1, which was in contact with the heater.

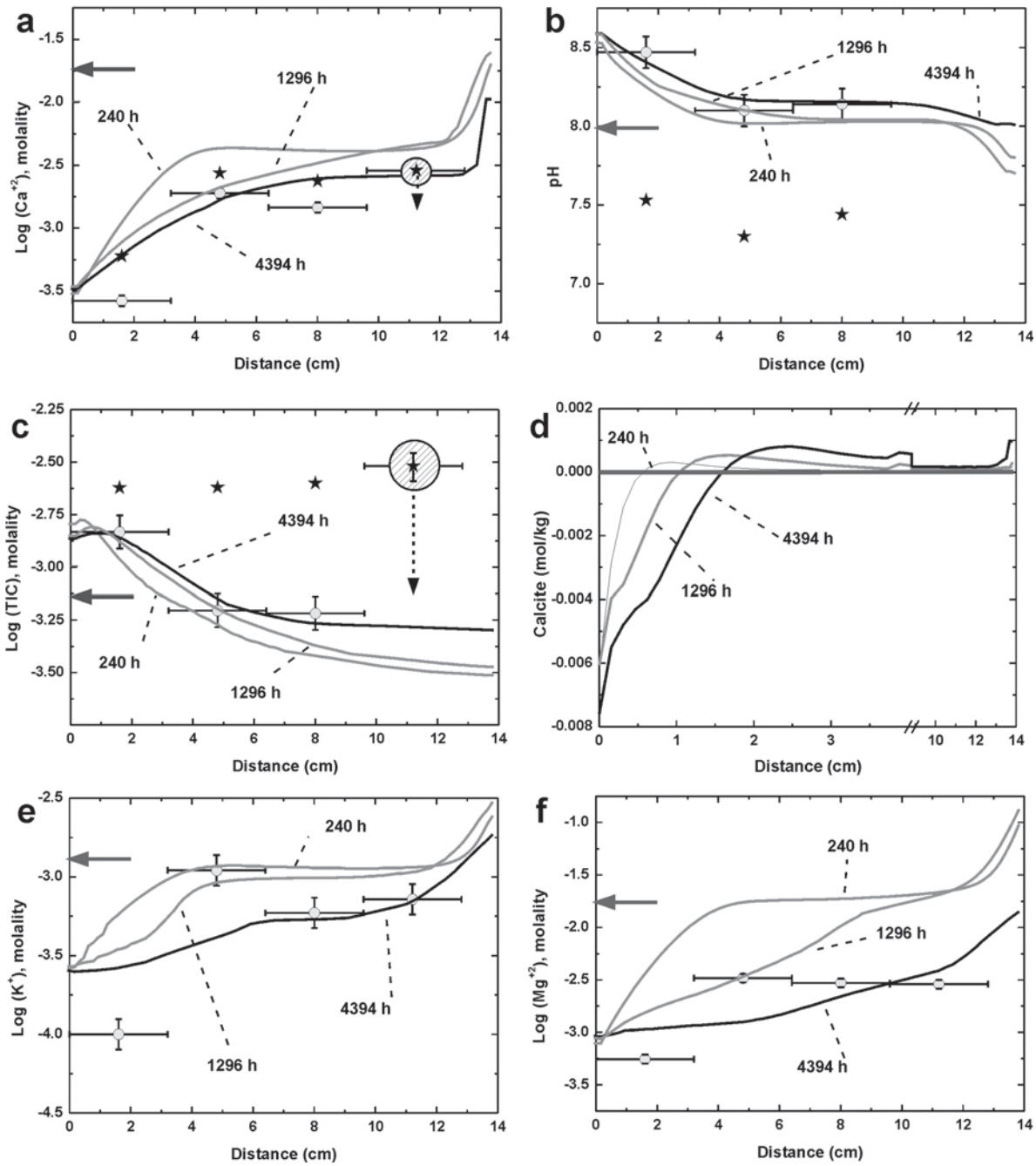

Figure 5. Experimental determinations and model results for different times (gray lines) and at the end of the experiment (black line). (a) Ca concentration; (b) pH; (c) concentration of total inorganic carbon; (d) mass of calcite dissolved/precipitated (negative/positive); (e) potassium concentration; (f) magnesium concentration. Arrows indicate the initial concentrations of the corresponding component. Black stars in plots a, b, and c represent uncorrected analytical values (see text). Circles with a dashed arrow in plots a and c indicate the direction of the correction if it had been performed.

Due to the entry of water and the dissolution of calcite in the areas near the hydration source, the pH increased in relation to the initial value (Figure 3c). The pH decreased close to the heater due to the increases in temperature and precipitation of calcite. However, as the water front approached this area, the pH increased again in response to the dissolution of the calcite. Furthermore, the model is consistent with the experimental data (Figure 5a,b,c) even in the case of section 2, where *P* and *T* corrections could not be performed.

Within the experimental time frame, the chemical composition of the exchange complex varied insignificantly (Figure 6a–d). In fact, the analytical uncertainties masked the recognition of any clear descriptive tendency. The modeling suggested some interesting patterns of change associated with the mechanisms of mass transfer outlined previously, *i.e.* transport and dissolution/precipitation reactions. Hence, except on the heater side, the amount of exchanged Na tended to decrease, whereas Ca increased. Consistent with these observations, the aqueous concentration of Na tended to decrease over time, except near the heater, while Ca increased. Next to the heater, the concentration of Na in the bentonite increased and Ca decreased with hydration. This can be explained easily by considering that, in most of the cell, pore waters were being flushed by the hydration process and, at the same time, Na from the exchange complex was being transferred to the solution to keep the equilibrium constraint. The effect on Ca was, however, the opposite, as the equilibrium with calcite tended to make the total concentration of this element less variable. Thus, the exchange complex lost Na and gained Ca. On the heater side, the evaporation of the pore water and precipitation of calcite provoked the opposite behavior in the exchange complex. Potassium behaved in an identical manner to Na, which is reasonable, considering the similarity in the value of the Na/K and Na/Ca selectivity coefficients. Finally, the exchanged Mg did not undergo significant changes, although a slight drop close to the hydration side was observed, in keeping with the progressive flushing with distilled water. The behavior of the exchange complex was complicated by the fact that the system is non-isothermal and one of the exchangeable components, Ca, had variable concentrations depending on the equilibrium with calcite (which can dissolve/precipitate throughout the cell but never becomes exhausted) which, in turn, depended on temperature. The model predicts that, in the intermediate portion of the cell, the exchange complex would be Ca enriched, coinciding with the zone where a significant amount of calcite has precipitated.

In general, all the aqueous components (including pH and the exchange complex of the bentonite) are

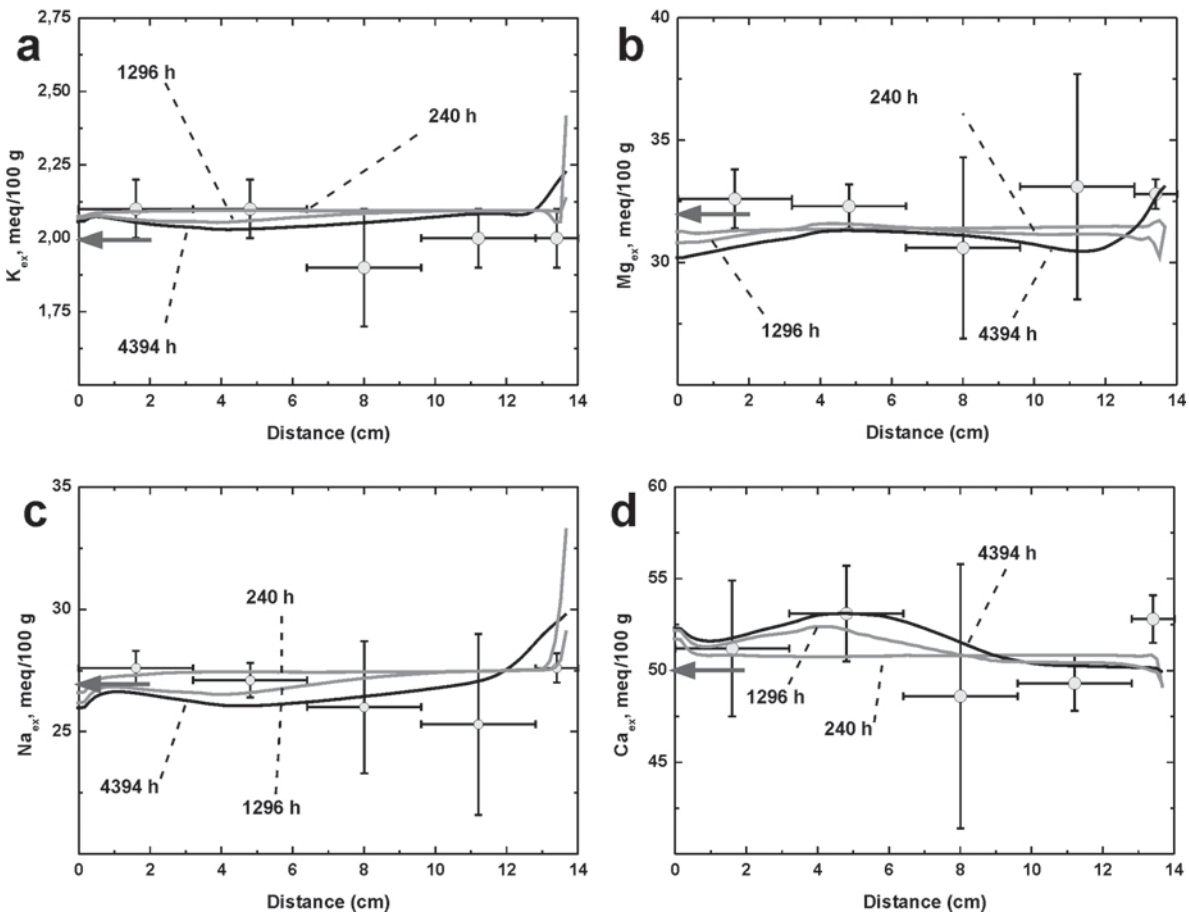

Figure 6. Experimental determinations and model results for different times (gray lines) and at the end of the experiment (black line). (a) Total exchanged K; (b) total exchanged Mg; (c) total exchanged Na; (d) total exchanged Ca. The arrows indicate the initial concentrations of the corresponding component.

reproduced reasonably well by the model. Section 4 (for K, Mg, and SO_4) and Section 5 (for K) are those found to be poorly reproduced, although the deviation of the model from the experimental results is within half an order of magnitude or less. Aside from the experimental uncertainties (which were addressed in another section), two additional explanations for these differences are offered: (1) heterogeneities in the bentonite, including the local concentration of mineral phases identified in trace amounts (dolomite, gypsum, barite, celestite, sulfides); and (2) kinetically constrained release of components linked to silicate or non-silicate phases. In either case, for the duration of the experiment, the kinetics of mineral dissolution/precipitation reactions did not appear to constrain significantly the evolution of the pore waters of the bentonite.

CONCLUSIONS

Modeling of the heating/hydration cell gives insights into the most significant processes occurring in the compacted bentonite within the restricted time frame of a 6-month period. Despite the experimental limitations inherent in the design (*i.e*. comparability with real repository conditions) and to the characterization of the soil (*i.e*. lack of data for different times, and limited availability of data at the end of the experiment), the results obtained are reproduced by the numerical model. The gas-pressure build-up (air-tight design), when computing the saturation of bentonite and the evaporation/condensation processes, plays a crucial role in the final distribution of water content. This is important because it has a significant impact on the geochemical subsystem.

The thermo-hydraulic model satisfactorily reproduces the geochemical results, *i.e*. the experimental values and tendencies of practically all components of the system as well as the associated water content. Hence, based on the comprehensive model and the set of available experimental data, the local equilibrium approach is acceptable for the description of the processes and evolution relevant to most of the components analyzed in the cell test (the research is currently limited to the study of the short term).

ACKNOWLEDGMENTS

The thermohydraulic cells were designed, constructed, run, and characterized at the CIEMAT (Research Center Energy, Environmental and Technological, Spain) by staff of the Department of Environmental Impact of Energy, under the direction of A. M. Fernández and M. V. Villar, to whom the authors are greatly indebted. This contribution benefited from discussions held at the FEBEX Working Groups and was carried out within the framework of FEBEX (I&II) research projects, funded by ENRESA (national waste company in Spain) and the RADWAS Program (radioactive waste program) of the EU (FI4W-CT95-00008; FIKW-CT-2000-0016). Special thanks to Dr F.J. Samper for the discussions during the preliminary developments of this work. Funding by the Spanish Ministry of Science and Technology (BIA2005-07916-C01/2; J. Delgado and V. Navarro), the Galician Government (PGIDIT02PXIC16201PN; J. Delgado), and the European Regional Development Funds 2007/2013 are also acknowledged. Comments and suggestions by Dr Joseph W. Stucki and two anonymous reviewers are greatly appreciated.

REFERENCES

Allison, J.D., Brown, D.S., and Novo-Gradac, K.J. (1991) *MINTEQA2/PRODEFA2, a geochemical assessment model for environmental systems*, version 3.0 user's manual. U.S. Environmental Protection Agency Report EPA/600/3-91/021.

Bear, J. (1972) *Dynamics of Fluids in Porous Media*. American Elsevier, New York, 764 pp.

Bethke, C.M. (1994) *The Geochemist 's Workbench*™, version 2.0, *A user's guide to Rxn, Act2, Tact, React, and Gtplot*. Hydrogeology Program, University of Illinois, USA.

Celia, M.A., Bouloutas, E.T., and Zarba, R.L. (1990) A general mass-conservative numerical solution for the unsaturated flow equation. *Water Resources Research*, **26**, 1483–1496.

Cheng, H.P. and Yeh, G.T. (1998) Development of a three-dimensional model of subsurface flow, heat transfer, and reactive chemical transport: 3DHYDROGEOCHEM. *Journal of Contaminant Hydrology*, **34**, 47–83.

Chillingarian, G.V. and Riecke, H.H. (1968) Data on consolidation of fine grained sediments. *Journal of Sedimentary Petrology*, **33**, 919–930.

Cuevas, J., Villar, M.V., Fernández, A.M., Gómez, P., and Martín, P.L. (1997) Pore waters extracted from compacted bentonite subjected to simultaneous heating and hydration. *Applied Geochemistry*, **12**, 473–481.

EC (2000) *Full-scale engineered barriers experiment for a deep geological repository for high level radioactive waste in crystalline host rock (FEBEX project)*. European Commission Report 19147_{EN}; 363 pp.

EC (2003) *Engineered Barrier Systems and the Safety of Deep Geological Repositories. State-of-the-art Report*. European Commission Report 19964_{EN}, 71 pp.

Edlefsen, N.E. and Anderson, A.B.C. (1943) Thermodynamics of soil moisture. *Hilgardia*, **15**, 31–298.

ENRESA (2004) *FEBEX II Project THG laboratory experiment*. ENRESATechnical Report 09/2004, 137 pp.

Fernández, A.M., Cuevas, J., and Rivas, P. (2000) Pore water chemistry of the FEBEX bentonite. Pp 577–588 in: *Scientific Basis for Nuclear Waste Management XXIV* (K.P. Hart and G.R. Lumpkin, editors). Materials Research Society Symposium Proceedings, **663**.

Fernández, A.M., Baeyens, B., Bradbury, M., and Rivas, P. (2004) Analysis of the pore water chemical composition of a Spanish compacted bentonite used in an engineered barrier. *Physics and Chemistry of the Earth*, **29**, 105–118.

Gens, A., García-Molina, A.J., Olivella, S., Alonso, E.E., and Huertas, F. (1998) Analysis of a full scale in situ test simulating repository conditions. *International Journal for Numerical and Analytical Methods in Geomechanics*, **22**, 515–548.

Huertas, F.J., Carretero, P., Delgado, J., Linares, J., and Samper, J. (2001) An experimental study on the ion-exchange behavior of the smectite of Cabo de Gata (Almería, Spain): FEBEX bentonite. *Journal of Colloids and Interface Science*, **239**, 409–416.

Johnson, J.W., Oelkers, E.H., and Helgeson, H.C. (1992) SUPCRT92: A software package for calculating the standard molal thermodynamic properties of minerals, gases, aqueous

species and reaction from 1 to 5000 bar and 0 to 1000ºC. *Computer & Geosciences*, **18**, 899–947.

Juncosa, R. (2001) *Modelos de flujo multifásico no isotermo y de transporte reactivo multicomponente en medios porosos*. ENRESA Technical Publication 01/2001, 287 pp.

Juncosa, R., Samper, J., Navarro, V., Delgado, J., and Carretero, P. (1999) Modelos de flujo multifásico no isotermo con reacciones químicas. Pp. 169–174 in: *Estudios de la Zona No Saturada* (R. Muñoz-Carpena, A. Ritter, and C. Tascón, editors). ICIA, Tenerife, Spain. http://carpena.ifas.ufl.edu/ZNS/4canarias/iv-05.pdf.

Juncosa, R., Samper, J., Vazquez, A., and Montenegro, L. (2003) Modelos de flujo multifásico no isotermo y transporte reactivo multicomponente en medios porosos: 2. Aplicación a bentonitas compactadas. *Ingeniería del Agua*, **10**, 37–48.

Juncosa, R., Xu., T., and Pruess, K. (2001) *A comparison of results obtained with two subsurface non-isothermal multi-phase reactive transport simulators, FADES-CORE and TOUGHREACT.* Ernest Orlando Lawrence Berkeley National Laboratory, Earth Sciences Division, California, USA, 37 pp.

KASAM (1995) *Nuclear Waste and the Environment. Proceedings of an International Seminar on Environmental Impact Assessment and its role in connection with the final disposal of nuclear waste*. The National Council for Nuclear Waste (KASAM), Luleå, Sweden, 24–26 October, 1994. SOU 1995,90.

Kaufhold, S., Dohrmann, R., Koch, D., and Houben, G. (2008) The pH of aqueous bentonite suspensions. *Clays and Clay Minerals*, **56**, 338–343.

Krumhansl, J.L. (1986) Observations regarding the stability of benonite backfill in a high-level (HLW) repository in rock salt. Sandia National Laboratory, Department of Energy, Alburquerque, NM, USA, 98 pp.

Li, Y. and Gregory, S. (1974) Diffusion of ions in sea water and in deep-sea sediments. *Geochimica et Cosmochimica Acta*, **38**, 703–714.

Lichtner, P.C., Steefel, C.I., and Oelkers, E.H. (editors) (1996) *Reactive Transport in Porous Media*. Reviews in Mineralogy, **34**. Mineralogical Society of America, Washington, D.C., 438 pp.

Lide, D.R. (1997) *Handbook of Chemistry and Physics*, 77th edition. The Chemical Rubber Company, CRC Press, Boca Raton, Florida, USA.

Manheim, F.T. (1974) Comparative studies on extraction of sediment interstitial waters: Discussion and comment on the current state of interstitial water studies. *Clays and Clay Minerals*, **22**, 337–343.

Mayer, K.U., Frind, E.O., and Blowes, D.W. (2002) Multicomponent reactive transport modeling in variably saturated porous media using generalized formulation for kinetically controlled reactions. *Water Resources Research*, **38**, 1174, pp. 13-1 to 13-21.

Mayhew, Y.R. and Rogers, G.F.C. (1976) *Thermodynamic and Transport Properties of Fluids*. Blackwell, Oxford, UK.

Millero, F.J. (1982) The effect of pressure on the solubility of minerals in water and sea water. *Geochimica et Cosmochimica Acta*, **46**, 11–22.

Milly, P.C.D. (1985) A mass-conservative procedure for time-stepping in models of unsaturated flow. *Advances in Water Resources*, **8**, 32–36.

Moore, D.M. and Reynolds, R.C. Jr. (1997) *X-ray Diffraction and the Identification and Analysis of Clay Minerals*. Oxford University Press, New York, 373 pp.

Muurinen, A. (2001) *Development and testing of analysis methods for bentonite pore water*. POSIVA working report 2001-07.

Navarro, V. (1997) Modelo de comportamiento mecánico e hidráulico de suelos no saturados en condiciones no isotermas. PhD thesis, Polytechnical University of Catalonia, Spain, 329 pp. (in Spanish).

Navarro, V. and Alonso, E.E. (2000) Modeling swelling soils for disposal barriers. *Computers and Geotechnics*, **27**, 19–43.

Nguyen, T.S., Selvadurai, A.P.S., and Armand, G. (2005) Modelling the FEBEX THM experiment using a state surface approach. *International Journal of Rocks Mechanics and Mining Sciences*, **42**, 639–651.

Nitao, J.J. (1998) *Reference manual for the NUFT flow and transport code, version 2.0*. Lawrence Livermore National Laboratory Report UCRL-MA-130651, California, USA, 55 pp.

NEA (1995) *The environmental and ethical basis of geological disposal of long-lived radioactive wastes. A collective opinion of the Radioactive Waste Management Committee of the OECD Nuclear Energy Agency*. OECD/NEA, Paris, 30 pp.

NEA (2000) Pore water extraction from argillaceous rocks for geochemical characterisation. Methods and Interpretation. OECD Nuclear Energy, Paris, 185 pp.

Olivella, S. (1995) Non-isothermal multiphase flow of brine and gas through saline media. PhD thesis, Polytechnical University of Catalonia, Spain, 197 pp.

Panday, S. and Corapcioglu, M.Y. (1989) Reservoir transport equations by compositional approach. *Transport in Porous Media*, **4**, 369–393.

Parkhurst, D.L. (1995) *PHREEQC, a computer model for speciation, reaction-path, advective transport and inverse geochemical calculations*. U.S. Geological Survey Water-Resources Investigations Report 80-96.

Pearson, F.J., Fisher, D.W., and Plummer, N.L. (1978) Correction of ground-water chemistry and carbon isotopic composition for effects of CO_2 outgassing. *Geochimica et Cosmochimica Acta*, **42**, 1799–1807.

Pollock, D.W. (1986) Simulation of fluid flow and energy transport processes associated with high-level radioactive waste disposal in unsaturated alluvium. *Water Resources Research*, **22**, 765–775.

Pruess, K. (1987) *TOUGH User's Guide*. Nuclear Regulatory Commission Report NUREG/CR–4645.

Pruess, K. (1991) *TOUGH2 A general-purpose numerical simulator for multiphase fluid and heat flow*. Earth Sciences Division, LWL, Berkeley, California, USA.

Pusch, R. and Karnland, O. (1986) *Aspects of the physical state of smectite-adsorbed water*. SKB Technical Report 86-25, Sweden, 59 pp.

Pusch, R., Muurinen, A., Lehikoinen, J., Bors, J., and Eriksen, T. (1999) *Microstructural and chemical parameters of bentonite as determinants of waste isolation efficiency*. European Commission. Nuclear Science and Technology, Project Report EUR 18950 EN.

Scanlon, B.R., Nicot, J.P., and Massmann, J.W. (2002) Soil gas movement in unsaturated systems. Pp. 297–341 in: *Soil Physics Companion* (A.W. Warwick, editor). CRC Press, Boca Raton, Florida, USA, 389 pp.

Simunek, J. and Suarez, D. (1994) Two-dimensional transport model for variably saturated porous media with major ion chemistry. *Water Resources Research*, **30**, 1115–1133.

Steefel, C.I. and MacQuarrie, K.T.B. (1996) Approaches to modelling of reactive transport in porous media. Pp. 83–129 in: *Reactive Transport in Porous Media* (P. Lichtner, C.I. Steefel, and E.H. Oelkers, editors). Reviews in Mineralogy, **34**. Mineralogical Society of America, Washington, D.C.

Stumm, W. and Morgan, J.J. (1981) *Aquatic Chemistry*, 2nd edition. Wiley-Interscience, New York, 780 pp.

Thomas, H.R. and He, Y. (1997) A coupled heat-moisture transfer theory for deformable unsaturated soil and its

algorithmic implementation. *International Journal for Numerical Methods in Engineering*, **40**, 3421–3441.

Van Genuchten, M.T. (1980) A closed-form equation for predicting the hydraulic conductivity of unsaturated soils. *Soil Science Society of America Journal*, **44**, 892–898.

Villar, M.V. and Lloret, A. (2004) Influence of temperature on the hydromechanical behavior of a compacted bentonite. *Applied Clay Science*, **26**, 337–350.

Villar, M.V., Cuevas, J., Martín, P.L., Campos, R., and Fernández, A.M. (1995) *Thermo-hydro-mechanical characterization of the Spanish reference clay material for engineered barrier for granite and clay HLW repository: laboratory and small mock-up testing*. ENRESA. Technical Publication 03/95.

Villar, M.V., Cuevas, J., and Martín, P.L. (1996) Effects of heater/water flow interaction on compacted bentonite: Preliminary results. *Engineering Geology*, **41**, 257–267.

Villar, M.V., Martín, P.L., and Barcala, J.M. (2005) Modification of physical, mechanical and hydraulic properties of bentonite by thermo-hydraulic gradients. *Engineering Geology*, **81**, 284–297.

Wang, H., Liang, D., Ewing, R.E., Lyons, S.L., and Quin, G. (2003) An improved numerical simulator for different types of flows in porous media. *Numerical Methods for Partial Differential Equations*, **19**, 343–362.

White, A.F. (1995) Multiphase non-isothermal transport of systems of reactive chemicals. *Water Resources Research*, **31**, 1761–1772.

Wolery, T.J. (1992) *EQ3/EQ6, a software package for geochemical modelling of aqueous systems, package overview and installation guide* (version 7.0). Lawrence Livermore Nacional Laboratory Report UCRL-MA-110662(1), California, USA.

Xu, T. (1996) Modelización del transporte no isotermo de sistemas de solutos reactivos a través de medios porosos parcialmente saturados. PhD thesis, University of A Coruña, Spain, 310 pp. (in Spanish).

Xu, T. and Pruess, K. (1998) *Coupled modeling of non-isothermal multi-phase flow, solute transport and reactive chemistry in porous and fractured media: 1. Model development and validation*. Ernest Orlando Lawrence Berkeley National Laboratory, Earth Sciences Division, California, USA.

Zilberbrand, M. (1999) On equilibrium constants for aqueous geochemical reactions in water unsaturated soils and sediments. *Aquatic Geochemistry*, **5**, 195–206.

(*Received 20 April 2009; revised 27 May 2010; Ms. 307; A.E. H. Stanjek*)